

Long time stress relaxation of amorphous networks under uniaxial tension: The Dynamic Constrained Junction Model

Haluk Konyali^{a,b}, Yusuf Menciloglu^a, Burak Erman^{c,*}

^a Sabanci University, Faculty of Engineering and Natural Sciences, Tuzla 34956, Istanbul, Turkey

^b Tekno Kauçuk, GOSB, İhsan dede cad. Gebze 41480, Kocaeli, Turkey

^c Koc University, Department of Chemical and Biological Engineering, Rumelifeneri Yolu, Sariyer 34450, Istanbul, Turkey

Received 5 November 2007; received in revised form 4 January 2008; accepted 7 January 2008

Available online 12 January 2008

Abstract

The constrained junction model that represents the stress–strain relations of amorphous networks in equilibrium is modified to analyze stress relaxation. Deviation of stress from equilibrium when a network is stretched suddenly is represented by a time dependent constraint contribution that is of the same form as that of the equilibrium theory. The time dependent motions of the junctions are assumed to obey the Langevin equation. The only new term in the model is a time dependent κ parameter that vanishes at long times. Results of the model are compared with uniaxial stress relaxation experiments on polyisoprene networks with different degrees of cross-linking. Experiments show that the time dependent κ parameter obeys a stretched exponential form, $\kappa(t) = \kappa_0 \exp[-(t/\tau)^\beta]$ with $\beta = 0.4$ and $\tau = 40$ s, both of which are the same for all extensions and cross-link densities studied. The front factor κ_0 depends on cross-link density in the same way as in the equilibrium case. Comparison with stress relaxation experiments shows satisfactory agreement at a wide range of extensions and for different degrees of cross-linking. The relatively low value of the stretched exponent parameter, $\beta = 0.4$, is interpreted in terms of a molecular picture where entanglements contribute to relaxation at a wide spectrum of time scales.

© 2008 Elsevier Ltd. All rights reserved.

Keywords: Dynamic Constrained Junction Model; Entanglements; Langevin dynamics

1. Introduction

When an amorphous polymeric network is stretched suddenly and kept at a fixed length, the force required to keep it at this length decreases until it reaches a finite value referred to as the force at equilibrium. The data in uniaxial tension are generally presented in terms of the reduced stress $[f^{*}] = f/A_0(\lambda - \lambda^{-2})$ where f is the force acting on the network, A_0 is the undeformed cross-sectional area, and λ is the extension ratio defined as the ratio of the final length to the original length of the sample. In uniaxial tension, the phenomenological Mooney–Rivlin equation describes the force extension relation satisfactorily over a wide range of deformations:

$$[f^{*}] = 2C_1 + \frac{2C_2}{\lambda} \quad (1)$$

where, $2C_1$ and $2C_2$ are the phenomenological coefficients which become functions of time when stress relaxation is considered [1]. The long time relaxation experiments of Ferry and Noordermeer [1], on lightly cross-linked polybutadiene networks showed that the time dependent Mooney–Rivlin equation describes the slow relaxation of uniaxial stress as well, with the observation that $2C_1$ relaxes fast and is approximately independent from $2C_2(t)$ which relaxes at a slower time scale. Eq. (1) serves as a good approximation both in equilibrium and out of equilibrium behavior of networks. In Fig. 1a and b, we present stress relaxation data from polyisoprene networks. The labels ‘Sample 1’ and ‘Sample 3’ refer to samples described in full detail below. The straight lines in the figures are the isochronous Mooney–Rivlin plots with time indicated on each

* Corresponding author. Tel.: +90 212 3381704; fax: +90 212 338 1548.

E-mail address: berman@ku.edu.tr (B. Erman).

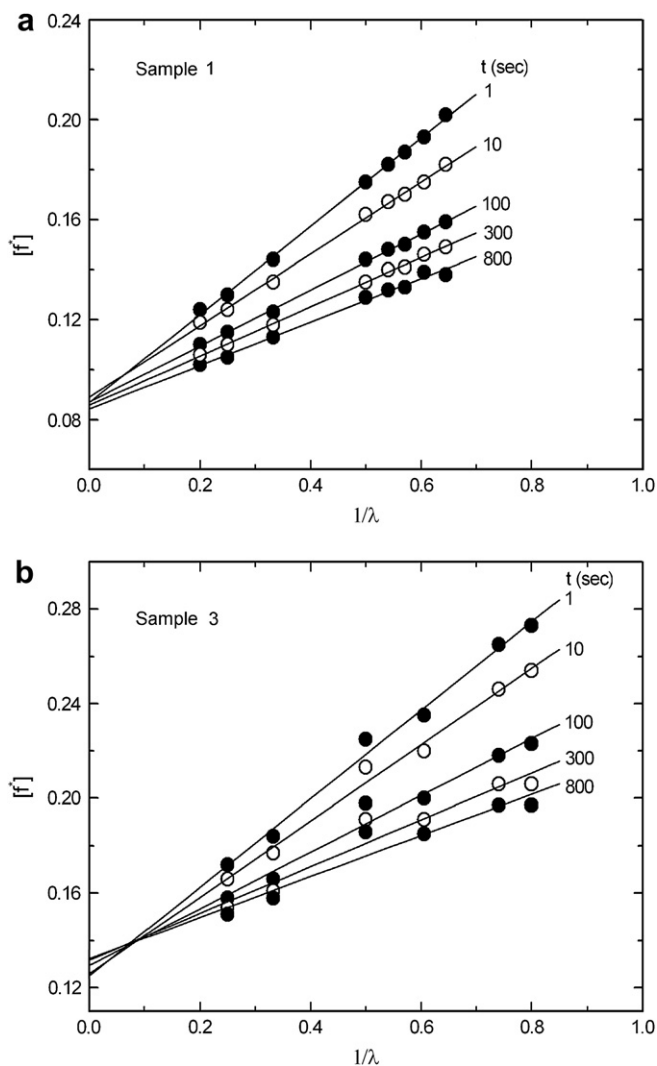


Fig. 1. Time dependent Mooney–Rivlin plots of two polyisoprene samples under uniaxial stress relaxation. (See Section 3 for details of the two samples.)

line. Points indicate the results of experiments. In agreement with Ferry's earlier observation, both figures show that the $2C_1$ value represented by the intercept is independent of time, and relaxation progresses through the decrease of $2C_2$.

In molecular interpretations of rubber elasticity, the $2C_1$ intercept is generally associated with contributions from the network cycle rank proportional to the number of chains constituting the network, and the slope $2C_2$ is associated with contributions from constraints that affect the fluctuations of junction points. Thus, the $2C_1$ term reflects contributions from network topology, whereas $2C_2$ reflects effects of constraints that suppress the fluctuations in the system. The molecular weight of the portion of a network chain between trapped entanglements is M_e . If the molecular weight of a network chain, M_c is much larger than M_e , then under sudden stretch, each subchain of molecular weight M_e will act as a transient network chain and will contribute to the stress similar to the contribution of the permanent junctions. The $2C_1$ term will be large, reflecting these transient contributions, and will subsequently decrease

upon relaxation. Thus, at shorter time scales, $2C_1$ exhibits time dependence and relaxation contains components from the transient entanglement network. The time scale of measurements shown in Fig. 1 is sufficiently large such that $2C_1$ is already time independent indicating that contribution of M_e 's has already died down and only the $2C_2$ component exhibits time dependence.

The contribution of entanglements to $2C_1$ has been the focus of both experimental and theoretical studies over the past several decades. Some experiments [2] show that at equilibrium, the effects of entanglements diminish at high extensions and/or high swelling ratios, and have no contribution to the $2C_1$ intercept. These are non-trapped entanglements or the so-called diffuse constraints. Others [3] show that contributions from chain entanglements trapped in the system during cross-linking do not relax fully and contribute to $2C_1$ [4]. The experiments of Rennar and Oppermann [5] showed the conditions under which trapped entanglements are important in a conclusive manner. In the present work, we specifically focus on the time independence of $2C_1$, and not on the nature of contributions to it.

Although the Mooney–Rivlin model is good in representing tension data, it fails under compression and other types of deformation in equilibrium, and is a phenomenological equation that does not describe the molecular basis of network behavior. The constrained junction models [6–9] have been satisfactory in explaining the molecular basis of force–deformation relations at equilibrium. In the present work, we propose the time dependent constrained junction model to describe the relaxation behavior of amorphous networks.

In the first section below, we present the time dependent constrained junction model, followed by an experimental validation of the theory. In the last section, we discuss in detail the molecular picture that leads to the observed strain dependence of long time relaxation, and compare our results with previous work.

2. Theory and the model

At equilibrium, a network junction exhibits large-scale fluctuations about its mean position. This is because the network chains covalently attached to the junction, which we call 'pendent chains' from hereon, exhibit large-scale diffusive motions about their equilibrium configurations. In a tetra-functional phantom network where there are no constraints to suppress junction fluctuations, mean squared fluctuations $\langle(\Delta R)^2\rangle$ of a junction are related to the mean squared end-to-end distance $\langle r^2\rangle_0$ of a network chain by [7] $\langle(\Delta R)^2\rangle = (3/8)\langle r^2\rangle_0$. For a polyisoprene network with reduced stress, $[f^*] = 0.1 \text{ Nmm}^{-2}$, the radius of the fluctuation domain for a junction at equilibrium is about 50 \AA and there are about 50 cross-links that share this domain. In real networks this sphere is smaller due to constraints. According to the constrained junction model [6,8], the mean squared radius of the domain in which a network junction fluctuates is inversely proportional to the constraint parameter, κ_0 . This parameter is defined as the ratio

$$\kappa_0 = \frac{\langle \Delta R^2 \rangle_0}{\langle \Delta s^2 \rangle_0} \quad (2)$$

where, $\langle \Delta R^2 \rangle_0$ is the mean square fluctuation of the junction in the phantom network and $\langle \Delta s^2 \rangle_0$ is the mean square fluctuations from the center of constraints. The value of κ_0 varies between 0 for highly cross-linked networks and about 10 or 12 for lightly cross-linked networks. If $\langle \Delta s^2 \rangle_0$ goes to zero, κ_0 goes to infinity, and the affine network model is recovered.

The diffusive motions of junctions have been observed in spin echo experiments [10]. These experiments, carried out on poly(dimethylsiloxane) networks with labeled junctions showed that the junctions move diffusively with characteristic relaxation times of 1–10 ns in a region whose size agrees with the predictions of the constrained junction model. The factors that affect the diffusion times of a junction come from its steric interactions with the entanglement domain and from the network chains that are covalently attached to it at the ϕ -functional junction.

According to the constrained junction model, the entanglement domains transform affinely with macroscopic deformation. In a deformed network at equilibrium, the constraint domain is affinely transformed. Given the sufficiently long time, a junction can explore all points in this domain, as shown by the spin echo experiments. At short times following a sudden stretch, the junction does not have a chance to explore all points available to it at equilibrium. It explores the small vicinity of its initial position during the moment of stretch. As the network is allowed to relax, however, the junction diffusively explores larger and larger regions of the constraint domain. Stated in another way, the size $\langle (\Delta s)^2 \rangle$ of the domain that appears in the definition of the κ_0 parameter, Eq. (2), in which the junction can fluctuate is small at short times following the stretch and spreads out as time progresses. Thus, the κ_0 parameter should be a function of time. The time dependent contributions to κ_0 are expected to be large at short times following the sudden stretch and vanish with time as equilibrium is approached. The process may be followed easily through the time dependence of the $2C_1$ and $2C_2$ parameters where the former reflects the dynamics operating below length scales of $[(M_e/M_c)\langle r^2 \rangle_0]^{1/2}$ while the latter reflects the dynamics at length scales of $\langle r^2 \rangle_0$ or larger. Here, $\langle r^2 \rangle_0$ is the mean squared end-to-end distance of the unperturbed network.

Based on the above discussion, we write the force $f(t)$ acting on the network at time t as

$$f(t) = f_{\text{ph}} + f_{\text{c,eq}} + f_{\text{c}}(t) \quad (3)$$

where f_{ph} is the component of force due to the phantom network, and $f_{\text{c,eq}}$ and $f_{\text{c}}(t)$ are the equilibrium and nonequilibrium forces due to constraints, respectively.

For uniaxial deformation [7],

$$f_{\text{ph}} = \left(\frac{\xi kT}{L_0} \right) \left(\lambda - \frac{1}{\lambda^2} \right) \quad (4)$$

Here, L_0 is the length of sample, and ξ is the cycle rank of the network denoting the number of chains that should be cut in order to reduce the network to a tree. The second term $f_{\text{c,eq}}$ in Eq. (3) is given by the constrained junction model as

$$f_{\text{c,eq}} = f_{\text{ph}} \left[\frac{\lambda K(\lambda) - \lambda^{-2} K(\lambda^{-1})}{\lambda^2 - \lambda^{-2}} \right] \quad (5)$$

where,

$$K(\lambda^2) = B \left[\frac{\dot{B}}{B+1} + \kappa_0^{-1} \frac{\lambda^2 \dot{B} + B}{B + \kappa_0 \lambda^{-2}} \right] \quad (6)$$

$$B = \kappa_0^2 \frac{\lambda^2 - 1}{(\lambda^2 + \kappa_0)^2} \quad (7)$$

$$\dot{B} = B \left[\frac{1}{\lambda^2 - 1} - \frac{2}{\lambda^2 + \kappa_0} \right] \quad (8)$$

The fundamental assumption of the theory of irreversible thermodynamics for small deviations from equilibrium is that the functional dependence of local entropy on the local extensive parameters is identical to the dependence in equilibrium [11]. This assumption allows us to extend the equilibrium constraint theory to the time domain, according to which the term $f_{\text{c}}(t)$ in Eq. (3) now reads as

$$f_{\text{c}}(t) = f_{\text{ph}} \left[\frac{\lambda K(\lambda^2, t) - \lambda^{-2} K(\lambda^{-1}, t)}{\lambda - \lambda^{-2}} \right] \quad (9)$$

where the time dependence is introduced to the K function as

$$K(\lambda^2, t) = B(t) \left[\frac{\dot{B}(t)}{B(t)+1} + \kappa(t)^{-1} \frac{\lambda^2 \dot{B}(t) + B(t)}{B(t) + \kappa(t) \lambda^{-2}} \right] \quad (10)$$

with

$$B(t) = \kappa(t)^2 \frac{\lambda^2 - 1}{(\lambda^2 + \kappa(t))^2} \quad (11)$$

$$\dot{B}(t) = B(t) \left[\frac{1}{\lambda^2 - 1} - \frac{2}{\lambda^2 + \kappa(t)} \right] \quad (12)$$

The parameter $\kappa(t)$ now becomes the only additional parameter to describe the relaxation behavior of the networks. The junction performs Brownian motion under the joint action of the pendent chains and the constraint domain. We assume that the pendent chains impose quickly varying forces on the junction relative to the response of the constraint domain. The latter provides the friction force. The motion of the junction may then be studied by the Langevin equation. In the Appendix, we show that the solution to the Langevin equation leads to the following form for the time dependent component of the κ parameter:

$$\kappa(t) = \frac{\kappa_0}{1 + \frac{t}{\tau_1} - \alpha(3 + 4e^{-(t/2\alpha\tau_1)} - e^{-(t/\alpha\tau_1)})} \quad (13)$$

where, κ_0 is the equilibrium value of the κ parameter, $\tau_1 = m\zeta\langle(\Delta s_0)^2\rangle/6kT$ has dimensions of time, $\alpha = 3kT/m\zeta^2\langle(\Delta s_0)^2\rangle$ is dimensionless, and $\zeta = 1/2\alpha\tau_1$ has dimensions of inverse time. When $t = 0$, $\kappa(0) = \kappa_0$, at short times it exhibits a double exponential decay, and at long times it decays as $\sim 1/t$, and becomes zero at infinite time.

In real networks, there are several relaxation pathways of different time scales that contribute to the time dependent κ parameter. In general these are such that the relaxation through one pathway depends on the prior relaxation through another pathway. These complex patterns of relaxation are not reflected by the simple Langevin formulation presented here. In order to introduce such dependencies, the functional form of $\kappa(t)$ should show more diffuse dependence on time. Two such possible forms are

$$\kappa(t) = \kappa_0 \exp\left[-\left(\frac{t}{\tau}\right)^\beta\right] \quad \kappa(t) = A\left(\frac{t}{\tau}\right)^{-m} \quad (14)$$

where, τ is the characteristic time of relaxation of constraint effects, β is the exponent, m is the power, and κ_0 and A are the front factors. The expression on the left in Eq. (14) is the stretched exponent form, and the one on the right is a power form, originally used by Chasset and Thirion [12] to describe the long time relaxation of natural rubber networks. The two functions exhibit significant differences, both at short and long times. The power relation diverges as time goes to zero. It shows much faster decay than the stretched exponent at short times, and much slower decay at long times. Comparison with experimental data, as will be discussed in more detail below, showed that the power relation does not represent relaxation satisfactorily whereas the stretched exponent shows almost perfect agreement with data. We therefore adopt the stretched exponent form. The solution to the Langevin equation leads to κ_0 which is identical to the corresponding equilibrium value so that Eq. (13) is recovered at $t = 0$. The stretch exponent β , indicating the multiexponential behavior of relaxation, is different than unity as will be shown in the experimental validation of the theory below.

The theoretical model presented in this section is valid only at long times at which the time dependence of the $2C_1(t)$ term has vanished. There are excellent theories of rubber viscoelasticity that describe the short time behavior in which the transient entanglement network contribution is significant [13].

In the following section, we present an experimental validation of the Dynamic Constrained Junction Model.

3. Experimental

3.1. Materials used

The raw materials used in this recipe were natural rubber (polyisoprene), zinc oxide, stearic acid, CBS (*N*-cyclohexyl-2-benzothiazole sulphenamide) and sulfur. All the raw materials were used as received. The natural rubber grade was Ribbed Smoked Sheet, RSS1, with a Mooney viscosity of 85 Mooney Units, MU, at 100 °C, $M_w \approx 350\,000$ and a polydispersity index

of 2.5. They were supplied from Eversharp Rubber Industries, Jalan, Singkang, Jementah, Johor. Zinc oxide, 99.7% purity with a 550 g/l bulk density was supplied from Metal Oksit (www.metaloksit.com). Stearic acid with an acid value 208.8 mg KOH/g, fatty acid composition 55.2% C16, 44.2% C18 was supplied from Natoleo (www.natoleo.co.kr). CBS was supplied from MLPC. Its melting point was 97 °C, ash content was 0.3% and specific gravity was 1.27. Sulfur was supplied from MLPC (www.mlpc-intl.com). Its melting point was 115 °C and specific gravity was 2.04.

3.2. Compounding

Compounds were prepared by using a lab scale 1.5 l Werner & Pfleiderer internal mixer. This internal mixer has standard tangential rotor geometry. The homogenizations were made on the two roll open mills. Rubber was fed into the chamber, masticated for 2 min and then zinc oxide and stearic acid were added. The compound was dumped at around 135 °C. It homogenized on the two roll mill for 5 min. In the second stage, accelerator and sulfur were added on the two roll mill for different compounds.

3.3. Vulcanization

Vulcanization was carried out in a compression molding with 160 t clamping force. All test sheets were vulcanized at 150 °C/35 min. The test sheet dimensions were 210 × 300 × 2 mm³.

Before the test sheets were vulcanized, rheometer curves were checked at 150 °C which is the temperature at which the test sheets were vulcanized later on. The rheometer curves showed that the torque values reach a plateau and remained constant from thereon, indicating that there is no reversion. The optimum cure times were obtained between 25 and 30 min depending on the different cross-linking densities in the rheometer curves. To be on the safe side, all sheets were vulcanized at 150 °C for 35 min knowing that there is no reversion for these recipes.

3.4. Relaxation tests

Dumbbell shaped test specimens of 2 mm thickness were cut out from the vulcanized sheets with the help of a Zwick sample cutter in accordance with DIN 53 504, S1, with dimensions ca. 50 × 10 × 2 mm³. Relaxation tests were carried out in a Zwick Roell Z2.5 universal tensile machine (UTM) with a load cell of 2.5 kN. Extension data were acquired at every 10 μm with an accuracy of 1%. The equipment used was testXpert V10.1 version software. Dumbbell shaped test sheets were tested at UTM with a pre-load of 0.2 N that prevented the initial curvature of the free samples. Test sheets were stretched to different extension ratios at a speed of 800 mm/min, and relaxed for 880 s for every sample. Data were taken at every 0.02 s during the test. In order to simplify presentation, we use the notation in Table 1 for sample designation.

Table 1
Sample notation

Sample number	M_c^a 10^4 (Da)	f_{ph}^b (MPa)	κ^b
1	1.32	0.092	9.0
2	1.12	0.104	8.0
3	0.86	0.132	6.0
4	0.75	0.154	4.6

^a Obtained from the equilibrium $2C_1$ values of force-deformation experiments.

^b Obtained from the fit of the equilibrium constrained junction model to experimental data.

4. Results

In Figs. 2–5, we present isochronous plots for networks with different cross-link densities. The ordinates denote the reduced stress $[f^*]$ and the abscissae are the reciprocal extension ratios. The points show the results of experiments. The shortest time of observation is 1 s. The longest time of 880 s recorded in the experiments did not correspond to full equilibrium, but sufficiently close to it for all of the samples. The curves are obtained from the theory presented in this paper. They are obtained for each figure as follows: first a value for κ_0 and $[f_{ph}^*]$ is assumed. We also assumed the stretched exponential form for the function $\kappa(t)$. For a given value of τ and β the calculated $[f^*]$ values are compared with $[f^*]$ values obtained from experiments. The calculations are repeated and the $(\kappa_0, [f_{ph}^*])$ and (τ, β) pairs that give the best agreement are accepted. Same procedure is repeated for each figure. The relaxation time of 40 s that gives the best agreement of theory with experiment is the same for all four samples. However, this is not true for lower cross-link densities and larger values of τ are required as elaborated in more detail in Section 5.

In Fig. 2, the data and theory show excellent agreement for all times up to extension ratios of 3. Beyond that point data remain above the theoretical curves, probably due to finite chain extensibility or crystallization effects that are not included in the theoretical model. Experimental data points show some

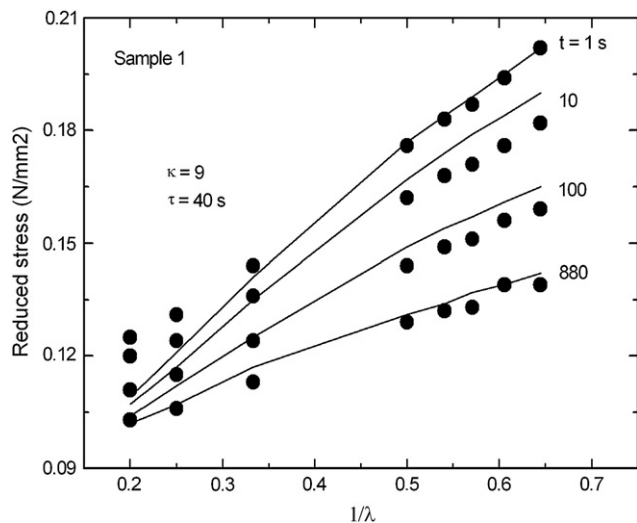


Fig. 2. Isochronous plots of Sample 1 and comparison with the Dynamic Constrained Junction Model results.

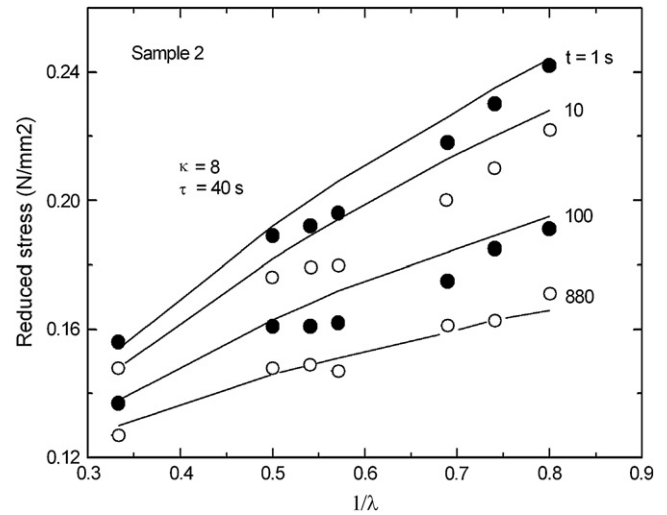


Fig. 3. Isochronous plots of Sample 2 and comparison with the Dynamic Constrained Junction Model results.

scatter in Fig. 5 due to difficulties of relaxation experiments on higher cross-link density samples.

In Figs. 6–9, the dependence of stress on time is presented for the four samples.

The extension ratios are indicated on each curve. Comparison of experimental points with results of the theory indicates that the model can accurately describe the time dependent behavior of networks in simple tension.

5. Discussion

In the present study, we extended the equilibrium constrained junction model to stress relaxation in uniaxial extension. In line with the fundamental assumption of irreversible thermodynamics, we took the functional dependence of the out of equilibrium stress on deformation same as given by the equilibrium theory. Results based on this simplification are in excellent agreement

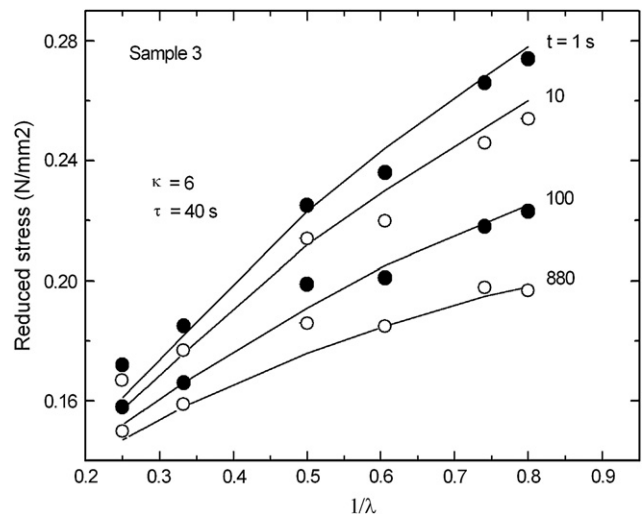


Fig. 4. Isochronous plots of Sample 3 and comparison with the Dynamic Constrained Junction Model results.

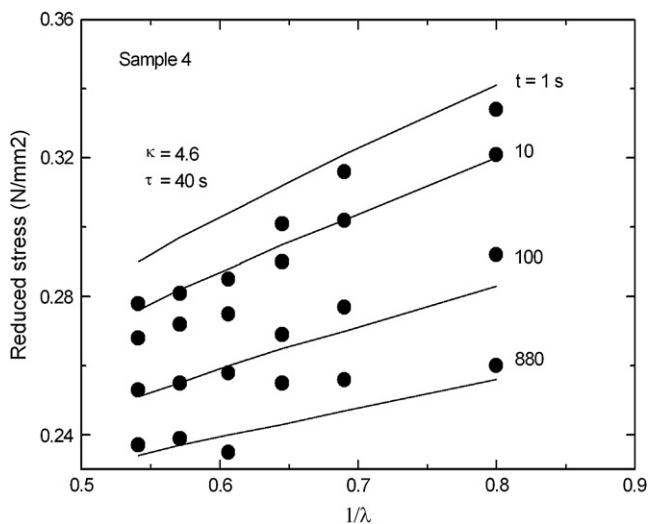


Fig. 5. Isochronous plots of Sample 4 and comparison with the Dynamic Constrained Junction Model results.

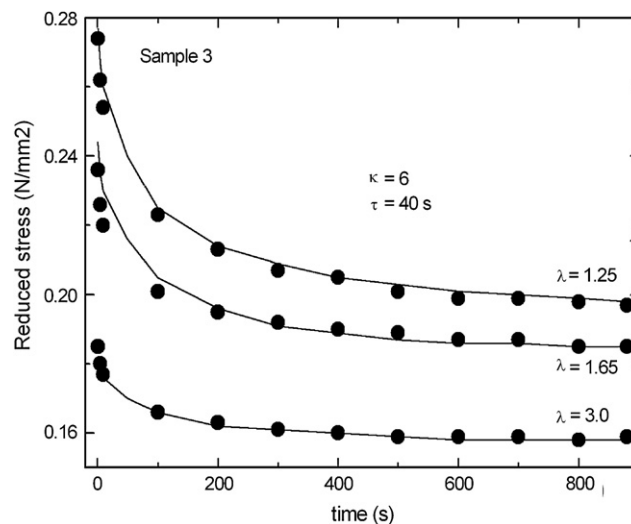


Fig. 8. Dependence of stress on time for Sample 3.

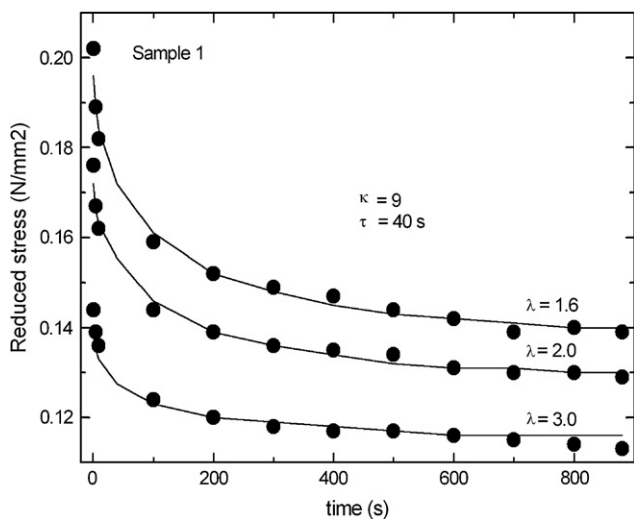


Fig. 6. Dependence of stress on time for Sample 1.

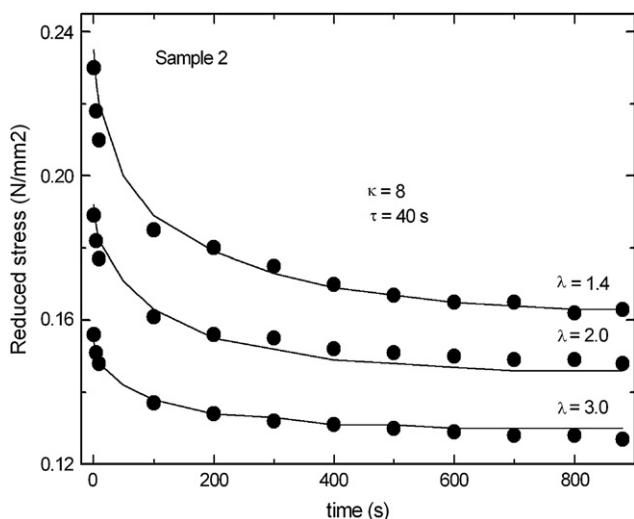


Fig. 7. Dependence of stress on time for Sample 2.

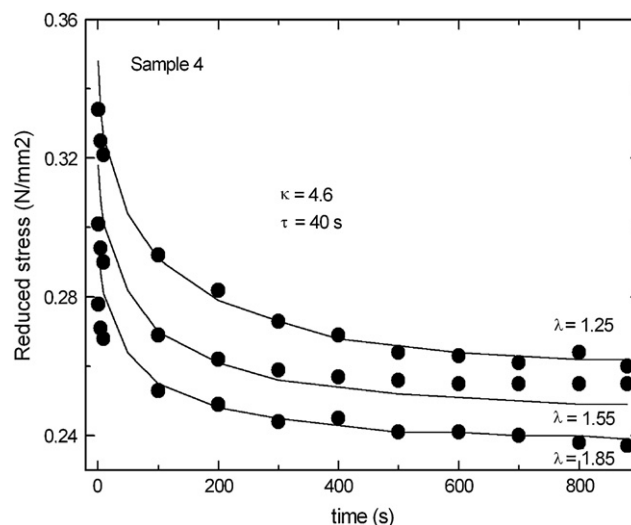


Fig. 9. Dependence of stress on time for Sample 4.

with experiment. Relaxation is described by a single parameter, $\kappa(t)$ which leads to experimental data only if it is of the stretched exponent form. This form, which is known as the Williams–Watts–Kohlrausch form in phenomenological theories, may be taken as an indication of serial cooperativity where different pathways of relaxation exist in which one relaxation step depends on the occurrence of another. Stated in another way, relaxation goes through hierarchically constrained steps: sudden stretching of the network causes an affine-like deformation of chains. Chains deformed in this manner do not relax all at once. A group of chains relax first, this induces the relaxation of others, through network connectivity. Thus, according to this interpretation, relaxation propagates from one junction to its topological neighbors in a serial fashion. We would like to indicate that this interpretation, although plausible, is one of several other possible relaxation pathways [14–22]. The stretch exponent type of hierarchical relaxation was introduced by Palmer et al. [23], and since then has been adopted for relaxation in a diverse field of materials.

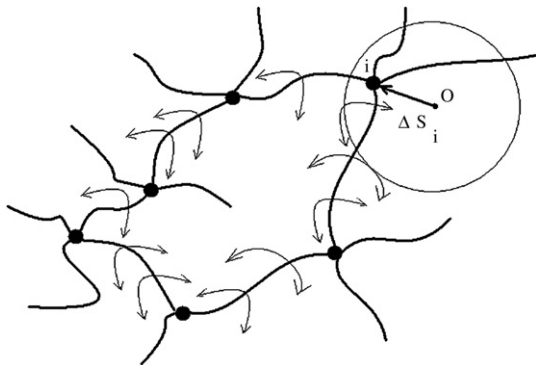


Fig. 10. Fluctuations of the junction i under the effects of entanglements.

In order to understand the molecular basis of long time relaxation, we consider the relaxation components of a junction in more detail: a junction is embedded into the ϕ -functional network by means of ϕ chains. The size of the fluctuation domain of the junction is determined by the fluctuations of the ϕ chains covalently attached to the junction, and the rest of the network to which these ϕ chains are attached. As briefly stated in Section 2, the system deforms close to affine when a sudden stretch is applied to the network. The chains and the junctions are close to ‘frozen’ at the initial state due to the hindrance of entanglements and steric effects. As the system relaxes, the junction explores different points in its fluctuation domain. We term this diffusional motion ‘the relaxation of the junction’. The excursions of the junction are obviously a result of the fluctuations of the pendent chains. The pendent chains perform their fluctuations under the presence of intermolecular effects, i.e., entanglements. The entanglements on chains can be transferred to the junction most pronouncedly if the junction is part of a cycle as shown in Fig. 10. In fact, in a perfect network, there are several cycles of different lengths that affect the fluctuations of a junction. In Fig. 10, a cycle of length 6 is shown. The circle shows the fluctuation domain of junction i . The center of this domain is indicated by O . The vector ΔS_i indicates the instantaneous fluctuation of the junction from its center. The distribution of ΔS_i will be time dependent in a relaxing network. This time dependent distribution will vanish as equilibrium is approached. Cycles of different lengths are expected to contribute differently to the relaxation of the junction. Longer cycles are subject to larger number of chain entanglements and hence their contribution to relaxation will be spread over longer time scales. Shorter cycles with only a few entanglements will be the fastest relaxation contributors. If the relaxation time associated with a cyclic path is τ_i and the contribution of this path to relaxation is $g(\tau_i)$, then the stretched exponential form, may be written as

$$e^{-(t/\tau)^\beta} = \sum_i g(\tau_i) e^{-(t/\tau_i)} \quad (15)$$

where the left hand side is determined by the experimentally obtained τ and β . Once these parameters are known, the distribution function $g(\tau_i)$ may be calculated by [24]

$$g(\tau_i) = \frac{1}{\pi\tau} \sum_{k=1}^{\infty} \frac{(-1)^k}{k!} \sin(\pi\beta k) \Gamma(\beta k + 1) \left(\frac{\tau_i}{\tau}\right)^{\beta k} \quad (16)$$

Here, $\Gamma()$ is the gamma function. For $\beta = 0.4$ and $\tau = 1$ s, the distribution function is calculated from Eq. (16) and is shown in Fig. 11. The peak contribution is equal to 0.175 and its relaxation time is around $\tau_i = 2$ s. The relaxation times are spread over a large range. Even at a relaxation time of 20 s, the amplitude is 0.06 which is significant. According to the molecular model described above, such large relaxation times are those that result from entanglements along long cyclic paths.

We would like to point out that the independence of the characteristic time τ from cross-link density is due to the small range of cross-link densities used in the experiments as may be readily seen from Table 1. The M_c of polyisoprene is 6750. Accordingly, M_c/M_e values vary between 1 and 2 for Samples 1–4. A possible interpretation that the same relaxation time characterizes all of the four samples is due to the small range of M_c/M_e for these samples. For lower degrees of cross-linking, the independence of τ from cross-link density does not hold, as expected. In Fig. 12, we present results on a sample of lower cross-link density in which $M_c/M_e = 3$. During the time scale of observation, the $2C_1$ parameter of this sample exhibited time dependence that is of the same order of magnitude as that of $2C_2$. This may be seen from the short time region of Fig. 12 where the theoretical curves cannot follow the rapid decay of experimental points due to the decay of $2C_1$. The decay of $2C_1$ with time is not included in the model. Thus, the present model is valid only for time scales where $2C_1$ has become independent of time, and in this region, the relaxation behavior may be described by the same characteristic time of $\tau = 40$ s for the cross-link densities shown in Table 1.

In 1965, Chasset and Thirion performed the first long time relaxation measurements on stretched natural rubber [12] and proposed the power relation

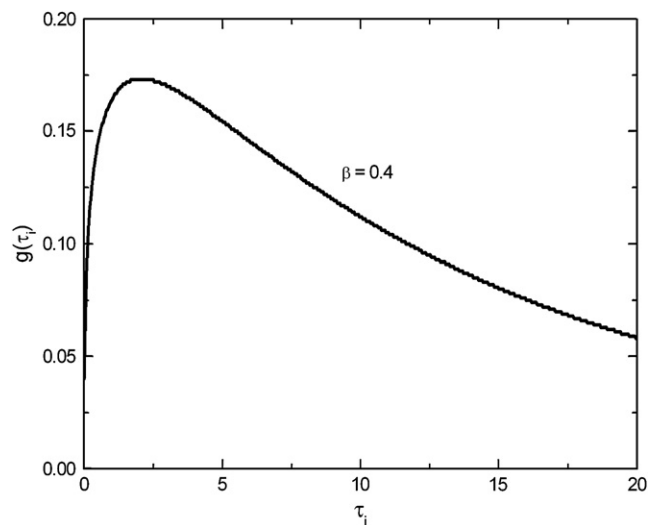


Fig. 11. The spectrum of relaxation times for the exponent $\beta = 0.4$.

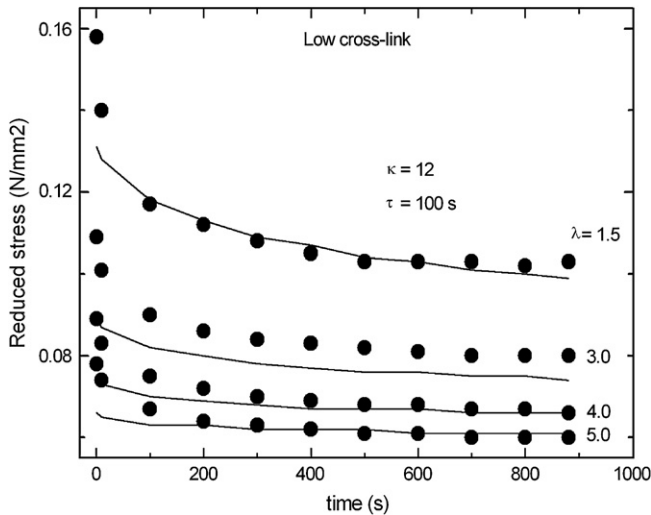


Fig. 12. Relationship of stress with time for low cross-link density sample.

$$E(t) = E(0) \left[1 + \left(\frac{t}{\tau} \right)^{-m} \right] \quad (17)$$

as a satisfactory approximation to the relaxation modulus $E(t)$. Later, a theoretical basis for the long time relaxation was proposed by Curro and Pincus [14] who proposed that relaxation resulted from the relaxation of the dangling chains. This interpretation is based on the single chain reptation concept of deGennes [25] where one end of a chain is fixed at a stationary point and the remaining part reptates in the presence of topological constraints. Curro and Pincus summed up the contributions to the relaxation modulus from different dangling chains and arrived at the Chasset–Thirion expression for the relaxation. In a later paper, Curro et al., [15] extended the reptation theory by modifying the Pearson–Helfand model for polymer stars [26] and showed that their model agrees with the Curro–Pincus model and the Chasset–Thirion expression at long times. Gaylord and DiMarzio proposed [16] an alternative relaxation mechanism, based on the hopping model of hindered diffusion. This model lead to the stretched exponent form of the relaxation function rather than the Chasset–Thirion power relation. In a later paper, McKenna and Gaylord showed that the power law relation works only over a limited time, with deviations from experimental data at long times [17]. Havranek and Heinrich assumed a stretch exponent relaxation function to describe the time dependent behavior [18]. In a theoretical analysis, Sommer found that the tail end of relaxation obeys the stretched exponent form with an exponent of 1/3. Heinrich and Vilgis made a critical review of the different predictions and pointed out to the common origin of the stretched exponent and power expressions [19]. Thirion and Monnerie used double step stretching experiments to test the reptation of dangling chains [20,21] and proposed that pendent chains as well as junction constraints both contribute to the stress relaxation of networks. Batra et al. [22] performed relaxation experiments on end-linked polydimethylsiloxane elastomers with long pendent chains to test the validity of the empirical Chasset–Thirion equation and found that this functional form holds only in an intermediate time regime of the relaxation spectrum.

In order to compare the results of the present model with those given in earlier literature, we present in Fig. 13, $\kappa(t)$ values as a function of time obtained by using the stretched exponent and the power relations. The circles are obtained from Eq. (13) by taking $\kappa_0 = 10$, $\tau_1 = 8$, and $\alpha = 1.0$. The solid curve is obtained by the stretched exponent function of Eq. (14) by taking $\kappa_0 = 10$, $\tau_1 = 12$, and $\beta = 0.4$. The values of κ_0 and τ_1 are chosen to obtain the best agreement with the calculated points. The dashed curve is obtained by the power relation given in Eq. (14), by taking $A = 10$, $\tau = 0.1$, and $m = 0.4$. Comparison of the curves shows that the results obtained using the stretched exponent form agrees with the results of Eq. (13) over a wide time span. Inasmuch as the stretched exponent form agrees perfectly with experimental data on natural rubber, we can conclude that the solution of the Langevin equation is satisfactory. The power form, on the other hand, decays very fast for short times and very slowly for long times when compared with the Langevin equation solution. The different choices of A , τ and m lead to agreement with experiment either at very short times or at long times, but a satisfactory solution that would give agreement over the full range was not possible.

The time dependent component of the stress for small deformations is obtained from Eq. (9) as

$$f_c(t) \approx \frac{(\kappa(t)^2 + 1)}{(\kappa(t) + 1)^4} \kappa(t)^2 \quad (18)$$

Thus, the time dependent force decays with the square of $\kappa(t)$. This leads to the stretched exponent $f_c(t) \sim \exp[-(t/\tau')^\beta]$ and the Chasset–Thirion power relation $f_c(t) \sim (t/\tau)^{-2m}$ for the force at small deformations. Thus, the functional relation of force to time can be taken, similar to that of $\kappa(t)$, as the stretch exponent or the Chasset–Thirion form. Since the Chasset–Thirion relation was not satisfactory in representing $\kappa(t)$, it is not expected to perform well for the force–time relation. Thus, the conclusion of McKenna and Gaylord [17] and Batra et al.

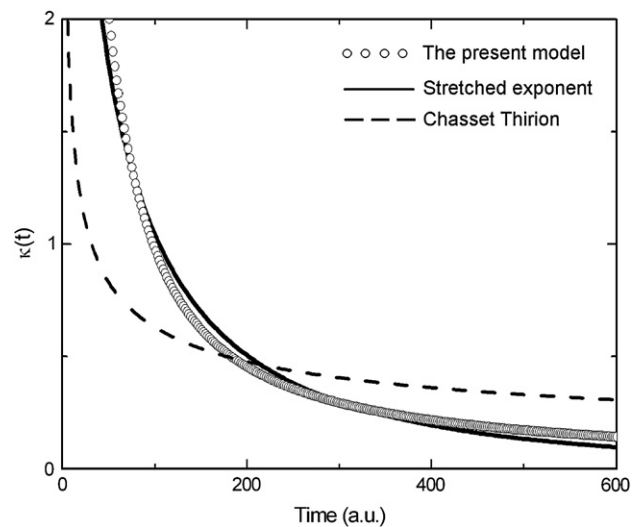


Fig. 13. Comparison of $\kappa(t)$ obtained from different representations presented as a function of time in arbitrary units.

[22] on the inadequacy of the Chasset–Thirion form over large time spans is also a consequence of the present work.

As a final remark it should be pointed out that the equilibrium constrained junction model can satisfactorily describe multiaxial stress–strain behavior of networks whereas the Mooney–Rivlin model fails [27]. Along these lines, extension of the present Dynamic Constrained Junction Model to relaxation in multiaxial states of deformation may lead to a better description of network viscoelasticity under general loading.

Appendix

The distribution of the fluctuations Δs of junctions from their centers of entanglements is modified when a network is stretched suddenly. At small times following the stretch, the junction will be embedded in their immediate environments. Thus the distribution of Δs will transform close to affine at initial times. As time progresses, the junctions will explore larger regions as a result of diffusive motions, and in the absence of network connectivity, the magnitude of fluctuations will become indefinite. Thus, the time dependent component of Δs will be executing Brownian motion, governed by the Langevin equation [28]

$$\frac{d\dot{\Delta s}}{dt} = -\zeta\dot{\Delta s} + A(t) \quad (\text{A1})$$

where, $\dot{\Delta s}$ is the time rate of change of Δs . $A(t)$ is the fluctuating force on the junction, and ζ is the friction force. The formal solution of Eq. (A1) is

$$\dot{\Delta s} = \dot{\Delta s}_0 e^{-\zeta t} + e^{-\zeta t} \int_0^t e^{\zeta t'} A(t') dt' \quad (\text{A2})$$

The displacement Δs is obtained by integration as

$$\Delta s = \Delta s_0 + \int_0^t \dot{\Delta s}(t') dt' \quad (\text{A3})$$

Substituting Eq. (A2) into Eq. (A3) leads to

$$\Delta s = \Delta s_0 + \zeta^{-1} \dot{\Delta s}_0 (1 - e^{-\zeta t}) + \int_0^t \zeta^{-1} [1 - e^{-\zeta(t-t')}] A(t') dt' \quad (\text{A4})$$

The fluctuations Δs are Gaussianly distributed [28]

$$W(\Delta s, t; \Delta s_0, \dot{\Delta s}_0) = \left[\frac{m\zeta^2}{2k\pi T(2\zeta t - 3 + 4e^{-\zeta t} - e^{-2\zeta t})} \right]^{3/2} \times \exp - \left[\frac{m\zeta^2 (\Delta s - \Delta s_0 - \zeta^{-1} \dot{\Delta s}_0 (1 - e^{-\zeta t}))^2}{2kT(2\zeta t - 3 + 4e^{-\zeta t} - e^{-2\zeta t})} \right] \quad (\text{A5})$$

where, $W(\Delta s, t; \Delta s_0, \dot{\Delta s}_0)$ is the probability that the junction is at position Δs from its mean location at time t , given that it was at Δs_0 at time zero with an initial velocity of $\dot{\Delta s}_0$, and m is an effective mass representative for the junction. For sufficiently long times, neglecting the effects of initial velocity and taking the ensemble average yields

$$\langle (\Delta s)^2 \rangle = \langle (\Delta s_0)^2 \rangle + \frac{3kT}{m\zeta^2} (2\zeta t - 3 + 4e^{-\zeta t} - e^{-2\zeta t}) \quad (\text{A6})$$

which leads to the time dependent κ parameter

$$\kappa(t) = \frac{\langle (\Delta R)^2 \rangle}{\langle (\Delta s)^2 \rangle} = \frac{\langle (\Delta R)^2 \rangle}{\langle (\Delta s_0)^2 \rangle + \frac{3kT}{m\zeta^2} (2\zeta t - 3 + 4e^{-\zeta t} - e^{-2\zeta t})} \quad (\text{A7})$$

At $t=0$, the righthand side becomes $\langle (\Delta R)^2 \rangle / \langle (\Delta s_0)^2 \rangle$ which is the equilibrium κ , κ_0 . At long times, fluctuations $\langle (\Delta s)^2 \rangle$ grow indefinitely, and $\kappa(t)$ goes to zero, indicating that the time dependent component of stress resulting from constraints on the junction vanishes. The righthand side of Eq. (A7) shows that the relaxation of $\kappa(t)$ is not single exponential. In the long time approximation, the term linear in time dominates and Eq. (A7) may be approximated by

$$\kappa(t) = \frac{\kappa_0}{1 + (t/\tau)} \quad (\text{A8})$$

where,

$$\tau = \frac{\zeta}{6kT} \quad (\text{A9})$$

is the characteristic relaxation time. Eq. (A8) corresponds to slow relaxation. Based on the discussion of contributions to relaxation at different time and length scales, we approximate $\kappa(t)$ by a stretched exponential function, given by Eq. (14).

References

- [1] Noordermeer JWM, Ferry JD. *J Polym Sci Polym Phys Ed* 1976;14:509–20.
- [2] Erman B, Wagner W, Flory PJ. *Macromolecules* 1980;13:1554–8.
- [3] Graessley WW. *Polymeric liquids and networks: structure and properties*. New York: Taylor and Francis; 2007.
- [4] Langley NR, Polmanteer KE. *J Polym Sci Polym Phys Ed* 1974;12:1023–34.
- [5] Rennar N, Oppermann W. *Colloid Polym Sci* 1992;270:527–36.
- [6] Flory PJ. *J Phys Chem* 1977;66:5720–9.
- [7] Erman B, Mark JE. *Structures and properties of rubberlike networks*. New York: Oxford University Press; 1997.
- [8] Erman B, Flory PJ. *Macromolecules* 1982;15:806–11.
- [9] Flory PJ, Erman B. *Macromolecules* 1982;15:800–6.
- [10] Ewen B, Richter D. In: Mark JE, Erman B, editors. *Elastomeric polymer networks*. Englewood Cliffs, NJ: Prentice Hall; 1992. p. 220–34.
- [11] Callen HB. *Thermodynamics and an introduction to thermostatistics*. New York: Wiley; 1985.
- [12] Chasset R, Thirion P. In: *Proceedings of the conference on physics of non-crystalline solids*, vol. 264; 1965. p. 345–59.
- [13] Ferry JD. *Viscoelastic properties of polymers*. New York: Wiley; 1980.
- [14] Curro JG, Pincus P. *Macromolecules* 1983;16:559–62.
- [15] Curro JG, Pearson DS, Helfand E. *Macromolecules* 1985;18:1157–62.

- [16] Gaylord RJ, DiMarzio EA. *Polym Bull* 1984;12:29–32.
- [17] McKenna BG, Gaylord RJ. *Polymer* 1988;29:2027–32.
- [18] Heinrich G, Havranek A. *Prog Colloid Polym Sci* 1988;78:1–9.
- [19] Heinrich G, Vilgis TA. *Macromolecules* 1992;25:404–7.
- [20] Thirion P, Monnerie L. *J Polym Sci Polym Phys Ed* 1986;24:2307–18.
- [21] Thirion P, Monnerie L. *J Polym Sci Polym Phys Ed* 1987;25:1033–41.
- [22] Batra A, Cohen C, Archer LA. *Macromolecules* 2005;38:7174–80.
- [23] Palmer RG, Stein DL, Abrahams E, Anderson PW. *Phys Rev Lett* 1984;53:958–61.
- [24] Lindsey CP, Patterson GD. *J Chem Phys* 1980;73:3348–57.
- [25] de Gennes PG. *Scaling concepts in polymer physics*. Ithaca, New York: Cornell University Press; 1979.
- [26] Pearson DS, Helfand E. *Macromolecules* 1984;17:888–95.
- [27] Erman B. *J Polym Sci Polym Phys Ed* 1981;19:829–35.
- [28] McQuarrie DA. *Statistical mechanics*. New York: Harper and Row; 1976.